ORGANOMETALLICS

Article

pubs.acs.org/Organometallics

Carbon−Carbon Bond Formation Reactivity of a Four-Coordinate NHC-Supported Iron(II) Phenyl Compound

Yuesheng Liu,[†] Jie Xiao,[†] Lei Wang,[†] You Song,[‡] and Liang Deng*,[†]

[†]State Key Laboratory of Organometallic Chemistry, Shanghai Institute of Organic Chemistry, Chinese Academy of Sciences, 345 Lingling Road, Shanghai, People's Republic of China 200032

[‡]State Key Laboratory of Coordination Chemistry, School of Chemistry and Chemical Engineering, Nanjing University, Nanjing, People's Republic of China 210093

Supporting Information

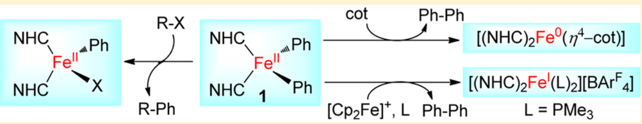

ABSTRACT: The preparation and characterization of a NHC-coordinated (NHC = N-heterocyclic carbene) ferrous phenyl complex $[(IPr_2Me_2)_2FePh_2]$ (**1**; IPr_2Me_2 = 1,3-diisopropyl-4,5-dimethylimidazol-2-ylidene) as well as its C−C bond formation reactivity have been studied. The four-coordinate iron(II) phenyl complex was prepared from the reaction of ferrous chloride with PhMgBr and IPr_2Me_2. It reacts with nonactivated primary and secondary alkyl bromides and chlorides to furnish cross-coupling products and the iron(II) monophenyl species $(IPr_2Me_2)_2FePhX$ (X = Br (**2**), Cl). When it is treated with cyclooctatetraene (cot) or $[Cp_2Fe][BAr^F_4]$ in the presence of PMe_3, it undergoes coordination or one-electron oxidation induced reductive elimination of biphenyl to form the corresponding iron(0) or iron(I) species $[(IPr_2Me_2)_2Fe(\eta^4\text{-cot})]$ (**3**) or $[(IPr_2Me_2)_2Fe(PMe_3)_2][BAr^F_4]$ (**4**). All of these iron-containing products have been fully characterized by various spectroscopic methods. Complex **1** and $(IPr_2Me_2)_2FeCl_2$ catalyze the reaction of $n\text{-}C_8H_{17}Br$ with (*p*-tolyl)MgBr to afford the cross-coupling product in moderate yields (49% and 47%), whereas the reactions employing **4** and **1**/PMe_3 as catalysts give the cross-coupling product in very low yields. The results reflect the complexity of the reaction mechanism of iron-catalyzed coupling reactions.

INTRODUCTION

The rapid development of iron-catalyzed organometallic transformations in recent years has raised fundamental questions about the identiies of their organoiron intermediates, which have remained largely undisclosed.[1] Iron phenyl species are among the most popular organoiron intermediates proposed in iron-catalyzed cross-couplings and consequently have attracted considerable recent interests.[2] In a pioneering work, Fürstner et al. reported the isolation and structural characterization of the anionic ferrous complex $[Li(Et_2O)_2]$-[Li(1,4-dioxane)]$[FePh_4]$ from the reaction of $FeCl_2$ with PhLi but thought it irrelevant to the catalytic process because of its propensity to eliminate biphenyl.[3] On the other hand, Nakamura, Nagashima, et al. found that the bulky aryl species $(TMEDA)Fe(Mes)_2$ (TMEDA = *N*,*N*,*N*′,*N*′-tetramethylethylene-1,2-diamine), which may emulate its phenyl analogue, can react with $n\text{-}C_8H_{17}Br$ to produce the cross-coupling product and proposed the catalytic relevance of iron(II) phenyl species.[4a] Fürstner, Neidig, and their co-workers recently found that the bis(phosphine)-supported iron(II) mesityl species $(P_2)Fe(Mes)_2$ (P_2 = 1,2-bis(diethylphosphino)ethane (depe), 1,2-bis(bis(3′,5′-di-*tert*-butylphenyl)phosphino)-benzene (SciOPP)) can also react with alkyl halides to produce cross-coupling products.[4b,c] Different from Nakamura's view, Bedford et al. thought that iron-catalyzed reactions with smaller aryl Grignard reagents should have a low-valent iron species as the catalytically active species since the authors noticed that the reactions of $FeCl_3$ with (*p*-tolyl)MgBr could lead to the formation of iron nanoparticles or low-valent iron species, presumably iron(I).[5]

The aforementioned ambiguity warrants exploration of putative iron phenyl species.[6] In this context, we report herein the isolation, characterization, and reactivity of the four-coordinate iron(II) phenyl complex $[(IPr_2Me_2)_2FePh_2]$. This NHC-supported iron(II) phenyl complex is stable at room temperature and can readily react with nonactivated alkyl halides to form monophenyl iron(II) complexes and cross-coupling products in high yields. Further studies on its tendency to undergo coordination and one-electron oxidation induced decomposition revealed that the latter reaction can readily take place to afford biphenyl and iron(I) species. These results, in addition to the different catalytic performances of the isolated iron(II) and iron(I) complexes in promoting the reaction of $n\text{-}C_8H_{17}Br$ with (*p*-tolyl)MgBr, suggest the complexity of the reaction mechanism of iron-catalyzed coupling reactions.

RESULTS AND DISCUSSION

Preparation and Characterization of the Iron(II) Diphenyl Complex. The wide use of monodentate NHC ligands in iron-catalyzed cross-coupling reactions[7,8] stimulated our interests in accessing relevant organoiron intermediates.[9] To seek pertinent models of iron phenyl species with

Received: October 22, 2014

DOI: 10.1021/om501061b

monodentate NHC ligation, we examined the reactions of $(NHC)_2FeCl_2$ (NHC = IPr_2Me_2; IMes = 1,3-bis(2′,4′,6′-trimethylphenyl)imidazol-2-ylidene) with 2 equiv of PhMgBr in THF. Both reactions could produce orange solutions, and from the reaction with $(IPr_2Me_2)_2FeCl_2$ we succeeded in the isolation of the phenyl complex $[(IPr_2Me_2)_2FePh_2]$ (**1**) as yellow crystals in 77% yield.[10] Alternatively, **1** was also prepared from the one-pot reaction of $FeCl_2$ with IPr_2Me_2 (2 equiv) and PhMgBr (2 equiv) in comparable yield (Scheme 1).

Scheme 1. Preparation Routes for 1

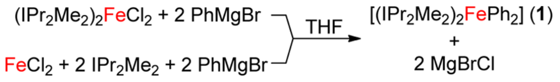

A single-crystal X-ray diffraction study has established the molecular structure of **1** as a four-coordinate iron(II) diphenyl species with a distorted-tetrahedral FeC_4 core (Figure 1a). The Fe−C(carbene) and Fe−C(phenyl) distances are typical of four-coordinate high-spin iron(II) species.[11] The ^1H NMR spectra of **1** recorded in THF-d_8 and C_6D_6 are similar and feature heavily broadened paramagnetically shifted resonances. The measured magnetic susceptibilities by SQUID exhibit μ_{eff} values ranging from 4.60 to 5.04 μ_B at 30−300 K, which is comparable to the spin-only value of 4.90 μ_B for a high-spin $S = 2$ state (Figure S1, Supporting Information).[12] The isomer shift ($\delta = 0.47$ mm/s) and quadrupole splitting ($\Delta E_Q = 2.38$ mm/s) analyzed from its zero-field ^{57}Fe Mössbauer spectrum measured at 80 K (Figure 1b) are consistent with those of related four-coordinate high-spin iron(II) species, such as $[(depe)Fe(Mes)_2]$ (0.39 and 1.71 mm/s)[13] and the tris(NHC) iron(II) complex $[(N(CH_2CH_2(C_3N_2MesH_2))_3)Fe(N_3)][BPh_4]$ (0.69 and 2.27 mm/s),[14] corroborating its high-spin ferrous nature.

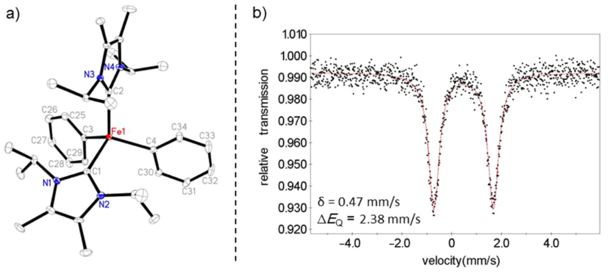

Figure 1. Molecular structure of **1** (left) showing 30% probability ellipsoids and partial atom schemes and its zero-field Mössbauer spectrum recorded at 80 K (right). Selected distances (Å) and angles (deg): Fe1−C1 2.162(2), Fe1−C2 2.157(2), Fe1−C3 2.090(2), Fe1−C4 2.091(2); C1−Fe1−C2 114.0(1), C3−Fe1−C4 113.3(1).

Reactions of the Iron(II) Diphenyl Complex with Organic Halides. Under a dinitrogen atmosphere, **1** does not show noticeable decomposition when its solutions (THF, Et_2O, and benzene) and the solid were kept at room temperature for days. Its stability under ambient conditions made a further reactivity study possible. Similarly to the bulky aryl complexes $(L_2)Fe(Mes)_2$ (L_2 = TMEDA, depe, SciOPP) and $[Fe(Mes)_3]^-$,[4,5] the four-coordinate iron(II) phenyl compound can react with the alkyl bromides n-$C_8H_{17}Br$ and c-$C_7H_{13}Br$ to produce the corresponding cross-coupling products in high yields (Table 1). More intriguingly, **1** can also react with the nonactivated alkyl chlorides n-$C_8H_{17}Cl$ and c-$C_7H_{13}Cl$ to give the corresponding cross-coupling products in 82% and 88% yields (Table 1). In these reactions, biphenyl, alkanes, and alkenes have been observed as the byproducts (Table 1).[15] The occurrence of alkanes and alkenes hints at a radical type mechanism for their carbon−halogen activation steps, which is further supported by the observation of the ring-opening product in the reaction of **1** with cyclopropylmethyl bromide (Table 1).[4]

Table 1. Reactions of 1 with Primary and Secondary Alkyl Halides[a]

$$(IPr_2Me_2)_2FePh_2 + R\text{-}X \xrightarrow[30\ ^\circ C,\ time]{THF} (IPr_2Me_2)_2FePhX + others$$

R-X	time [b]	yields (mmol) [c]			
n-$C_8H_{17}X$		n-C_8H_{17}-Ph	n-C_8H_{18}	n-C_8H_{16}	Ph-Ph
X = Br	6 h	0.081	0.010	0.003	0.033
X = Cl	12 h	0.082	0.005	0.008	0.013
c-$C_7H_{13}X$		c-$C_7H_{13}Ph$	c-C_7H_{14}	c-C_7H_{12}	Ph-Ph
X = Br	4 h	0.083	0.010	0.005	0.003
X = Cl	12 h	0.088	0.003	0.009	0.006
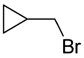	2 h	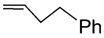 0.051			Ph-Ph 0.038

[a]Conditions: $(IPr_2Me_2)_2FePh_2$ (0.10 mmol) and halides (0.10 mmol) in THF (3 mL) at 30 °C with n-dodecane as the internal standard. [b]Time required for the full conversions of the halides. [c]GC yields.

In addition to the organic products, monophenyl iron(II) species in the form $(IPr_2Me_2)_2FePhX$ (X = Br, Cl) are the dominant iron-containing products. Figure S2 (Supporting Information) shows the ^1H NMR spectra of the reaction mixtures of **1** with n-$C_8H_{17}Br$, n-$C_8H_{17}Cl$, c-$C_7H_{13}Br$, and c-$C_7H_{13}Cl$. The similar peak patterns of the paramagnetically shifted resonances point out a common identity of the resulting iron-containing species $(IPr_2Me_2)_2FePhX$. Furthermore, a single-crystal X-ray diffraction study on the bromide complex $[(IPr_2Me_2)_2FePhBr]$ (**2**) that was independently prepared from the reaction of $FeBr_2$ with 2 equiv of IPr_2Me_2 and 1 equiv of PhMgBr in THF has unambiguously confirmed its structure (Figure 2a). The ^{57}Fe Mössbauer isomer shift of **2** (0.58 mm/s) is between those of **1** (0.47 mm/s) and Meyer's bis(NHC)-iron(II) dibromides (0.73−0.81 mm/s).[11c] Along with $(IPr_2Me_2)_2FePhX$, a small amount of $(IPr_2Me_2)_2FeX_2$ was also observed according to the ^1H NMR spectra (Figure S2, Supporting Information). The iron(II) dihalide complexes might come from the further cross-coupling reactions of $(IPr_2Me_2)_2FePhX$ with the alkyl halides[4a] and/or the ligand

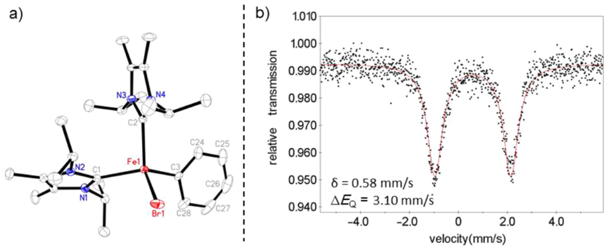

Figure 2. Molecular structure of **2** (left) showing 30% probability ellipsoids and partial atom schemes and its zero-field Mössbauer spectrum recorded at 80 K (right). Selected distances (Å) and angles (deg): Fe1−C1 2.130(2), Fe1−C2 2.140(2), Fe1−C3 2.108(2), Fe1−Br1 2.485(1); C1−Fe1−C2 100.4(1), C3−Fe1−Br1 109.4(1).

redistribution reaction of $(IPr_2Me_2)_2FePhX$ to $(IPr_2Me_2)_2FePh_2$ and $(IPr_2Me_2)_2FeX_2$.

Olefin Coordination and Oxidation Induced Biphenyl Reductive Elimination. Low-valent iron species were proposed as active intermediates in many iron-catalyzed cross-coupling reactions.[1,3,5,8d,16] With the aim to identify possible transformations of **1** to iron(0) and iron(I) species, we studied the decomposition reactions of **1** under different conditions.

Examining the interactions of **1** with some potential coordinating substrates, e.g. PPh_3, TMEDA, *n*-octene, fluorobenzene, chlorobenzene, and cyclooctatetraene (cot), revealed the inertness of **1** toward most of these compounds, except for cot. For the last case, slow formation of biphenyl was noticed[15] and the isolation of the iron(0) complex $[(IPr_2Me_2)_2Fe(\eta^4\text{-cot})]$ (**3**) (Scheme 2), whose structure is depicted in Figure 3a, confirmed the occurrence of olefin coordination induced biphenyl reductive elimination. The different outcomes of these reactions imply that coordination induced biphenyl reductive elimination from the iron(II) complex requires strong π-accepting ligands. Notably, olefin coordination induced C−C bond-forming reductive elimination is a well-known phenomenon for Ni(II), Pd(II), and Pt(II)[17] but is unprecedented for iron(II) species.[18]

Scheme 2. Reaction of 1 with cot

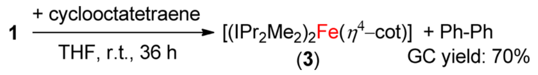

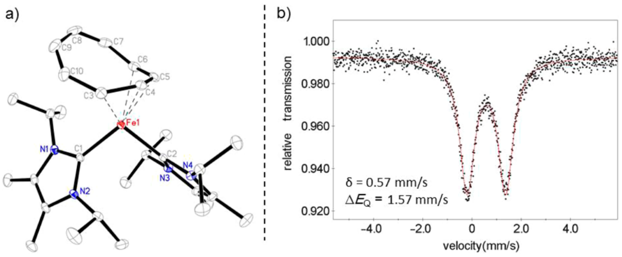

Figure 3. Molecular structure of **3** (left) showing 30% probability ellipsoids and partial atom schemes and its zero-field Mössbauer spectrum recorded at 80 K (right). Selected distances (Å) and angles (deg): Fe1−C1 1.995(1), Fe1−C2 2.005(1), Fe1−C3 2.161(1), Fe1−C4 2.073(1), Fe1−C5 2.065(1), Fe1−C6 2.423(1), C3−C4 1.414(2), C4−C5 1.424(2), C5−C6 1.416(2), C6−C7 1.426(2), C7−C8 1.370(3), C8−C9 1.419(3), C9−C10 1.355(2), C10−C3 1.446(2); C1−Fe1−C2 98.62(5).

Complex **3** was isolated as brown crystals. Its molecular structure established by XRD (Figure 3a) is close to that of $[(BAC)_2Fe(\eta^4\text{-cot})]$ (BAC = bis(diisopropylamino)-cyclopropenylidene) reported by Grubbs.[19] The η^4-bonded cot ligand in **3** has the bond lengths of the three metal-bound C−C bonds close to each other (1.414(2), 1.424(2), and 1.416(2) Å) and the Fe−C distances spanning a broad range (2.073(1)−2.423(1) Å). The Fe−C(carbene) bonds (2.00 Å on average) are longer than their congeners in $[(BAC)_2Fe(\eta^4\text{-cot})]$ (1.94 Å on average)[19] but shorter than those in $[(IEt_2Me_2)_2Fe(\eta^2\text{:}\eta^2\text{-dvtms})]$ (2.08 Å on average; IEt_2Me_2 = 1,3-diethyl-4,5-dimethylimidazol-2-ylidene, dvtms = divinyltetramethyldisiloxane).[20] The ^{57}Fe Mössbauer spectrum of **3** can be fitted with the parameters of δ = 0.57 mm/s and ΔE_Q = 1.57 mm/s (Figure 3b). The increased isomer shift in comparison to δ = 0.47 mm/s for $[(IEt_2Me_2)_2Fe(\eta^2\text{:}\eta^2\text{-dvtms})]$[20] suggests the enhanced metal-to-alkene π back-donation in the cot complex. Thus, **3** could also be viewed as a formal iron(0) species. The measured solution magnetic moment for **3** is 3.4(1) μ_B, which is close to that of our previously reported formal iron(0) alkene complexes, e.g. 3.5 μ_B for $[(IEt_2Me_2)_2Fe(\eta^2\text{:}\eta^2\text{-dvtms})]$ and $[(IMes)Fe(\eta^2\text{:}\eta^2\text{-dvtms})]$, and larger than the spin-only value of 2.83 μ_B for an S = 1 system. The large magnetic moment might be due to the presence of a large unquenched orbital moment contribution, as noted in other low-coordinate iron complexes.[21]

The potential of **1** to perform oxidation-induced decomposition was probed by both electrochemical and chemical oxidation studies. Cyclic voltammetry studies on a THF solution of **1** revealed that its oxidation can occur at quite negative potential with E_p = −0.53 V (vs SCE) and the process is irreversible (Figure S3, Supporting Information). This potential is lower than that of 0 V for the $[(IMes)_2FeCl_2]^{0/+}$ process,[11d] being consistent with the stronger electron-donating nature of phenyl anion versus chloride. The irreversibility implies the instability of the resultant iron(III) species $[(IPr_2Me_2)_2FePh_2]^+$, which is different from the six-coordinate iron dialkyl compounds $[(bipyridine)_2FeR_2]^+$, which are stable at 0 °C.[22]

Scheme 3. Reaction of 1 with Ferrocenium Cation in the Presence of PMe_3

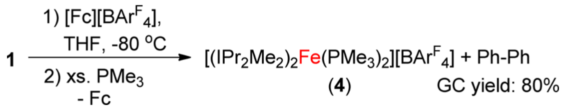

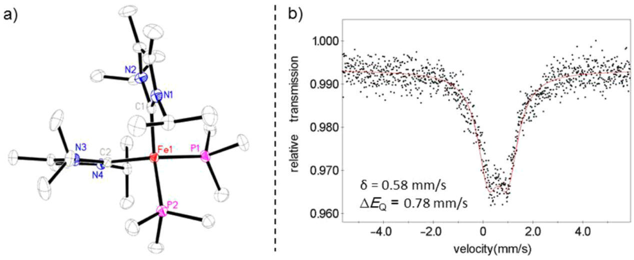

Figure 4. Molecular structure of the cation in **4** (left) showing 30% probability ellipsoids and partial atom schemes and the zero-field Mössbauer spectrum of **4** recorded at 80 K (right). Selected distances (Å) and angles (deg): Fe1−C1 2.081(6), Fe1−C2 2.079(5), Fe1−P1 2.305(2), Fe1−P2 2.318(2); C1−Fe1−C2 103.9(2), P1−Fe1−P2 99.14(7), C1−Fe1−P1 104.0(2), C1−Fe1−P2 122.8(2), C2−Fe1−P1 122.9(2), C2−Fe1−P2 105.7(2).

For the chemical oxidation reaction of **1** with 1 equiv of $[Cp_2Fe][BAr^F{}_4]$ in THF, GC analysis indicated the instant formation of biphenyl in 80% yield. The isolation of the resulting iron species was validated by the addition of 4 equiv of PMe_3 to the reaction mixture, from which the iron(I) complex $[(IPr_2Me_2)_2Fe(PMe_3)_2][BAr^F{}_4]$ (**4**) was obtained in 80% yield (Scheme 3). The structure of the iron(I) cation in **4** is shown in Figure 4a. The iron center is bonded with two IPr_2Me_2 and two PMe_3 ligands to form a distorted-tetrahedral geometry. In comparison to the Fe−C(carbene) distances in **1** and **3**, those in **4** (2.08 Å in average) are in the middle. The Fe−P distances are comparable to those in [PhB(CH$_2$PPr$^i_2$)$_3$Fe(PMe$_3$)].[23] In addition to this, the solution magnetic moment (4.3(1) μ_B) and the Mössbauer data (δ = 0.58 mm/s and ΔE_Q = 0.78 mm/s) of **4** are also similar to those of [PhB(CH$_2$PPr$^i_2$)$_3$Fe(PMe$_3$)].[23] These resemblances are indicative of the high-spin nature (S = $^3/_2$) of **4**.

Mechanistic Considerations of the Iron NHC Complex Mediated Cross-Coupling Reactions. The product pattern depicted in Table 1 suggests that the reactions of **1** with the alkyl halides are very likely proceeding in a single-electron transfer mechanism, as in the case of the reaction between (TMEDA)Fe(Mes)$_2$ and alkyl halides.[24] Considering the low reduction potentials of the nonactivated alkyl halides, which are generally lower than −1.5 V versus SCE on a glassy-carbon electrode[25] and significantly lower than the E_p value of −0.53 V for the irreversible oxidation of **1**, we thought that the reaction between R−X and the iron(II) phenyl species (IPr$_2$Me$_2$)$_2$FePh$_2$ or (IPr$_2$Me$_2$)FePh$_2$ should be an inner-sphere electron-transfer type, rather than an outer-sphere electron-transfer type. After the electron-transfer step (eq. 1 in Scheme 4), the resulting iron(III) intermediate could (i) interact with the alkyl radical to afford the cross-coupling product and the iron(II) monophenyl species (path a), (ii) react with iron(I) species formed by the interaction of the alkyl radical with an iron(II) diphenyl species to yield iron(II) products (path b), or (iii) undergo decomposition to furnish biphenyl and iron(I) species (path c). The combination of eqs 1 and 2 corresponds to a radical rebound mechanism,[2b] whereas the combination of eqs 1, 3, and 4 lead to a bimetallic oxidative addition pathway.[26] The observation of the cross-coupling products as the major products in Table 1 suggests that path c is not the dominant decomposition pathway for the iron(III) intermediate.

Scheme 4. Possible Mechanisms for the Reactions of 1 with Alkyl Halides

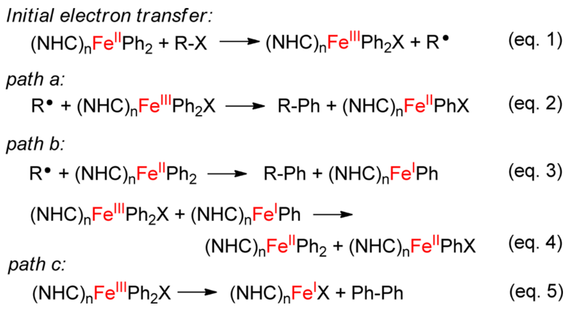

Prompted by the fine performance of **1** in the stoichiometric reactions with alkyl halides, we also studied its catalytic performance in promoting the cross-coupling of n-C$_8$H$_{17}$Br with (p-tolyl)MgBr, along with those of (IPr$_2$Me$_2$)$_2$FeCl$_2$ and **4** for comparison (Table 2). The reaction using 5 mol % of **1** can quickly produce a red-brown solution and white precipitate.[27] GC analyses indicated the formations of n-C$_8$H$_{17}$(p-tolyl), n-octane, and octenes in 49%, 13%, and 22% yields, respectively (entry 1, Table 2). Similar phenomena and product distribution were observed in the reaction with (IPr$_2$Me$_2$)$_2$FeCl$_2$ as catalyst (entry 2, Table 2). The catalytic reactions (entries 1 and 2) differ from the stoichiometric reaction (**1** with n-C$_8$H$_{17}$Br) in their faster rates, the decreased percentages of the cross-coupling product, and the increased percentages of the side products. The enhanced rates might be caused by the formation of the anionic species [(NHC)Fe(p-tolyl)$_3$]$^-$ or [Fe(p-tolyl)$_4$]$^{2-}$, whose anionic nature might render them highly reducing and enhance the redox reaction with n-C$_8$H$_{17}$Br. Recently, Bedford reported the observation of faster rates of [Fe(Mes)$_3$]$^-$ with organic halides versus that of the reaction with [(TMEDA)Fe(Mes)$_2$].[5] The increased percentages of the side products in the catalytic reactions (entries 1 and 2) may also relate to the formations of the anionic aryl iron(II) species, as Fürstner has noted that [FePh$_4$]$^{2-}$ is prone to oxidation-induced degradation to form biphenyl.[3]

Table 2. Iron NHC Complex Catalyzed Coupling Reactions of *p*-TolylMgBr with *n*-Octyl Bromide[a]

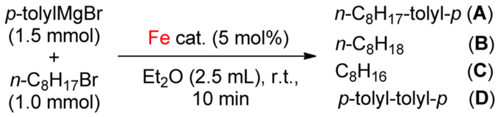

		yield (mmol)			
entry	catalyst	A	B	C	D
1	**1**	0.49	0.13	0.22	0.22
2	(IPr$_2$Me$_2$)$_2$FeCl$_2$	0.47	0.16	0.19	0.27
3	**4**[b]	0.09	0.18	0.35	0.28
4	**1** + PMe$_3$[c]	0.08	0.18	0.32	0.27

[a] Yields were determined by GC with n-dodecane as the internal standard and were averaged from two parallel experiments. [b] n-Hexadecane (0.09 mmol) was observed. [c] 25 mol % PMe$_3$. n-Hexadecane (0.09 mmol) was also observed.

When the iron(I) complex **4** was used as the catalyst, the yield of cross-coupling product dropped to 9%, and that of octenes increased to 35% (entry 3, Table 2). The catalytic reaction employing **1** and PMe$_3$ gave comparable results (entry 4, Table 2). The significantly decreased yields of cross-coupling products in entries 3 and 4 clearly indicate their distinct catalytic mechanism. While the effect of PMe$_3$ on the reaction mechanism has to wait for further examination, one could propose that the presence of PMe$_3$ might trigger catalytic cycles involving Fe(I) species.

CONCLUSION

The current study has shown that the selection of the suitable monodenatate NHC ligand enables the preparation of stable four-coordinate iron(II) diphenyl complex [(IPr$_2$Me$_2$)$_2$FePh$_2$]. Characterization data collectively pointed out the high-spin nature of the iron(II) phenyl complex in the solid state. Reactivity studies disclosed its versatile C−C bond-formation reactions.

The iron(II) phenyl complex [(IPr$_2$Me$_2$)$_2$FePh$_2$] can react with primary and secondary alkyl bromides and alkyl chlorides to afford cross-coupling products and monophenyliron(II) complexes (IPr$_2$Me$_2$)$_2$FePhX. The observation of alkenes and alkanes as the side products and the ring-opening product PhCH$_2$CH$_2$CH=CH$_2$ in the reaction with cyclopropylmethyl bromide suggests the single-electron-transfer character of the C−X bond cleavage step of these reactions. The interaction of [(IPr$_2$Me$_2$)$_2$FePh$_2$] with the good π-accepting ligand cot induces the formation of the iron(0) species [(IPr$_2$Me$_2$)$_2$Fe(η^4-cot)] and biphenyl, and the one-electron oxidation of [(IPr$_2$Me$_2$)$_2$FePh$_2$] could produce the iron(I) species and biphenyl. The use of PMe$_3$ as the coligand enables the isolation of the resulting iron(I) species in the form of [(IPr$_2$Me$_2$)$_2$Fe(PMe$_3$)$_2$][BAr$^F_4$]. The single-electron oxidation induced transformation suggests the propensity of iron(III) diphenyl species [(IPr$_2$Me$_2$)$_2$FePh$_2$]$^+$ to undergo biphenyl reductive elimination.

In addition to these, we also found that the iron(II) diphenyl compound is competitive in catalyzing cross-coupling of n-$C_8H_{17}Br$ with (p-tolyl)MgBr to give the cross-coupling product in moderate yield, along with substantial amounts of n-octene and n-octane. In contrast, the reaction catalyzed by $[(IPr_2Me_2)_2Fe(PMe_3)_2][BAr^F{}_4]$ gives the cross-coupling product in poor yield. The difference implies their distinct mechanisms. The differentiated rates of the catalytic and the stoichiometric reactions with n-$C_8H_{17}Br$ hint that $[(IPr_2Me_2)_2FePh_2]$ might be irrelevant to the catalytic cycle of the cross-coupling reaction. These results reflect the complexity of the reaction mechanism of iron-catalyzed coupling reactions.

EXPERIMENTAL SECTION

General Procedures. All experiments were performed under an atmosphere of dry dinitrogen with the rigid exclusion of air and moisture using standard Schlenk or cannula techniques or in a glovebox. All organic solvents were freshly distilled from sodium benzophenone ketyl immediately prior to use. $[(IPr_2Me_2)_2FeCl_2]$[28] and $[Cp_2Fe][BAr^F{}_4]$ (Ar^F = 3,5-bis(trifluoromethyl)phenyl)[29] were prepared according to literature methods. All chemicals were purchased from either Strem or J&K Chemical Co. and used as received unless otherwise noted. ^1H NMR spectra were recorded on a Varian Mercury 300 or 400 MHz spectrometer. All chemical shifts were reported in δ units with references to the residual protons of the deuterated solvents for proton chemical shifts. GC analyses were performed on a Shimadzu GC-2014 spectrometer. GC-MS analyses were performed on a Shimadzu GCMS-QP2010 Plus spectrometer. Elemental analysis was performed by the Analytical Laboratory of Shanghai Institute of Organic Chemistry (CAS). Magnetic moments were measured at 29 °C by the method originally described by Evans with stock and experimental solutions containing a known amount of $(CH_3)_3SiOSi(CH_3)_3$ standard.[30] Cyclic voltammetry measurements were made with a CHI 600D potentiostat in THF solutions using a sweep rate of 100 mV/s, a glassy-carbon working electrode, 0.1 M $[Bu_4N][PF_6]$ supporting electrolyte, and an SCE reference electrode. Under these conditions, $E_{1/2}$ = 0.55 V for the $[Cp_2Fe]^{0/+}$ couple. Absorption spectra were recorded with a Shimadzu UV-3600 UV−vis−NIR spectrophotometer. Magnetic measurements on the crystalline sample of **1** were carried out at an applied field of 2 kOe on a Quantum Design MPMP-XL7 superconducting quantum interference device (SQUID) magnetometer working in the temperature range 300−1.8 K. The molar magnetic susceptibilities were corrected for diamagnetism as estimated from Pascal's tables and for the sample holder by a previous calibration. The ^{57}Fe Mössbauer spectra were measured with a constant-acceleration spectrometer at 80 K. Low temperature was maintained by a CCS-850 Mössbauer Cryostat system (Janis Research Co.). Data were analyzed with MossWinn 4.0Pre (Beijing Shengtianjiayuan Keji Co.). Isomer shifts are relative to iron metal at room temperature.

X-ray Structure Determinations. The structures of the five compounds in Table S1 (Supporting Information) were determined. Crystallizations were performed at room temperature. Crystals were coated with Paratone-N oil and mounted on a Bruker APEX CCD-based diffractometer equipped with an Oxford low-temperature apparatus. Cell parameters were retrieved with SMART software and refined using SAINT software on all reflections. Data integration was performed with SAINT, which corrects for Lorentz−polarization and decay. Absorption corrections were applied using SADABS.[31] Space groups were assigned unambiguously by analysis of symmetry and systematic absences determined by XPREP. All structures were solved and refined using SHELXTL.[32] The metal and first coordination sphere atoms were located from direct-methods E maps; other non-hydrogen atoms were found in alternating difference Fourier synthesis and least-squares refinement cycles and during the final cycles were refined anisotropically. Hydrogen atoms were placed in calculated positions by employing a riding model. Final crystal parameters and agreement factors are reported in Table S1.

Preparation of $[(IPr_2Me_2)_2FePh_2]$ (1). *Method A.* To a suspension of $[(IPr_2Me_2)_2FeCl_2]$ (600 mg, 1.23 mmol) in THF/dioxane (20 mL/4 mL) was added a THF solution of PhMgBr (1.0 M, 2.7 mL, 2.7 mmol) at −78 °C. The resulting mixture was warmed to room temperature and stirred for 8 h, during which time the solution turned from colorless to yellow. After removal of the solvent, the residue was extracted with diethyl ether (15 mL × 3) and filtered. The filtrate was concentrated to about 15 mL. Slow evaporation of diethyl ether afforded **1** as yellow crystals (540 mg, 77%). Anal. Calcd for $C_{34}H_{50}FeN_4$: C, 71.56; H, 8.83; N, 9.82. Found: C, 71.43; H, 8.98; N, 10.15. Absorption spectrum (benzene): λ_{max}, nm (ε, M^{-1} cm^{-1}) 330 (4400), 1350 (130), 1480 (150). The ^1H NMR spectrum of this paramagnetic complex displayed two broad peaks in the range +150 to −150 ppm in C_6D_6. ^1H NMR (300 MHz, C_6D_6, 302 K): δ (ppm) 61.75, −6.72. Attempts to integrate the two peaks did not give a reasonable integration ratio. Dissolution of **1** in THF-d_8 also gave a yellow solution with a ^1H NMR spectrum similar to that observed in C_6D_6. ^1H NMR (300 MHz, THF-d_8, 302 K): δ (ppm) 66.35, −0.25.

Method B. $FeCl_2$ (300 mg, 2.37 mmol) and IPr_2Me_2 (860 mg, 4.73 mmol) were mixed in THF (25 mL), and the mixture was further stirred for 4 h at room temperature. To the suspension was added a THF solution of PhMgBr (1.0 M, 5.2 mL, 5.2 mmol) at −78 °C. The resulting mixture was warmed to room temperature and stirred overnight, during which time the solution turned from colorless to dark orange. After removal of the solvent, the residue was extracted with diethyl ether (25 mL × 3) and filtered. The filtrate was concentrated to about 20 mL. Recrystallization of the solution at −30 °C afforded **1** as yellow crystals (740 mg, 55%).

General Procedure for Reactions of 1 with n-$C_8H_{17}X$, c-$C_7H_{13}X$ (X = Br, Cl), and Cyclopropylmethyl Bromide. A dried Schlenk tube was charged with the alkyl halide (0.10 mmol), THF (3 mL), n-dodecane (0.10 mmol), and **1** (57 mg, 0.10 mmol) in a glovebox at room temperature. The reaction mixture was stirred at 30 °C, followed by GC.[15] During the course of the reaction, the solution slowly turned from yellow to orange (Figure S9, Supporting Information). When alkyl halide was consumed completely, a part of the reaction mixture was drawn and quenched with H_2O. The quenched mixture was extracted with diethyl ether and separated. The organic phase was then dried over $MgSO_4$, analyzed by gas chromatography−mass spectrometry (GC-MS) to confirm the identity of the products, and further analyzed by GC with a flame ionization detector (GC-FID) to quantify the yields with n-dodecane as the internal standard. The composition of the organic products is given in Table 1. Figure S6 (Supporting Information) shows the change in GC yields of the cross-coupling products versus time in the reactions of **1** with n-$C_8H_{17}X$ and c-$C_7H_{13}X$ (X = Br, Cl). Figure S7 (Supporting Information) depicts the organic product distribution over time in the reaction of **1** with n-$C_8H_{17}Br$ as the representative. On the other hand, the unquenched organic solution that was left was dried under vacuum and redissolved in C_6D_6. ^1H NMR analysis revealed the presence of characteristic ^1H NMR resonances of the monophenyl iron(II) species $(IPr_2Me_2)_2FePhX$ (X = Br, Cl), which are close to those of $[(IPr_2Me_2)_2FePhBr]$ (Figure S2, Supporting Information). In addition to the monophenyl complexes, the formation of small amounts of $(IPr_2Me_2)_2FeX_2$ (X = Br, Cl) was also noticed in the ^1H NMR spectra.

Preparation of $[(IPr_2Me_2)_2FePhBr]$ (2). $FeBr_2$ (400 mg, 1.86 mmol) and IPr_2Me_2 (690 mg, 3.82 mmol) were mixed for 4 h at room temperature in THF/dioxane (15 mL/3 mL). To the suspension was added a THF solution of PhMgBr (1.0 M, 1.9 mL, 1.9 mmol) at −78 °C. The resulting mixture was warmed to room temperature and stirred overnight, during which time the solution turned from colorless to light yellow. After removal of the solvent, the residue was extracted with THF (5 mL × 3) and filtered. The filtrate was concentrated to about 5 mL. Slow evaporation of THF afforded **2** as colorless crystals (850 mg, 80%). The coexistence of a small amount of $(IPr_2Me_2)_2FeBr_2$ in the products made the attempts to collect a satisfactory elemental analysis data unsuccessful. Anal. Calcd for $C_{34}H_{50}FeN_4$: C, 58.65; H, 7.91; N, 9.77. Found: C, 57.71; H, 7.90; N, 10.16. Absorption spectrum (benzene): λ_{max}, nm (ε, M^{-1} cm^{-1}) 330 (1660), 1464 (135). The ^1H NMR spectrum of this paramagnetic complex displayed four characteristic peaks in the range +150 to −150 ppm in C_6D_6. ^1H NMR (300 MHz, C_6D_6, 302 K): δ (ppm) 100.84 (2H), 18.65 (12H), 9.67 (24H), −34.91 (1H). Magnetic susceptibility (THF-d_8, 302 K): μ_{eff} = 5.0(1) μ_B.

Reaction of 1 with cot. To a solution of $[(IPr_2Me_2)_2FePh_2]$ (120 mg, 0.20 mmol) with *n*-dodecane (0.10 mmol) in THF (6 mL) was added cyclooctatetraene (cot; 21 mg, 0.20 mmol) at room temperature. The mixture was stirred at room temperature and followed by GC. Figure S8 (Supporting Information) shows the change in the GC yield of biphenyl versus time. After 36 h, the reaction mixture turned dark brown and the yield of biphenyl reached 70%. All volatiles were removed under vacuum. The brown residue was washed with *n*-hexane (2 mL), extracted with diethyl ether (2 mL × 3), and filtered. The filtrate was concentrated to about 3 mL. Slow evaporation of diethyl ether afforded $[(IPr_2Me_2)_2Fe(\eta^4\text{-cot})]$ (**3**) as brown crystals (69 mg, 66%). Anal. Calcd for $C_{30}H_{48}FeN_4$: C, 69.22; H, 9.29; N, 10.76. Found: C, 69.03; H, 9.15; N, 10.77. Absorption spectrum (benzene): λ_{max}, nm (ε, M^{-1} cm^{-1}) 360 (8800), 822 (250), 1340 (216). The ^1H NMR spectrum of this paramagnetic complex displayed four characteristic peaks in the range +150 to −150 ppm in C_6D_6. ^1H NMR (300 MHz, C_6D_6, 302 K): δ (ppm) 56.70, 9.39, 6.84, −95.29. Magnetic susceptibility (C_6D_6, 302 K): μ_{eff} = 3.4(1) μ_B.

Reaction of 1 with $[Cp_2Fe][BAr^F_4]$. To a solution of $[(IPr_2Me_2)_2FePh_2]$ (120 mg, 0.20 mmol) and *n*-dodecane (0.10 mmol) in THF (5 mL) was added a THF solution of $[Cp_2Fe][BAr^F_4]$ (220 mg, 0.20 mmol) at −80 °C. Immediately, the solution turned from yellow to orange. A THF solution of PMe_3 (61 mg, 0.80 mmol) was added to the mixture at the same temperature. The resulting mixture was warmed to room temperature. During the course of the reaction the color changed gradually from orange to yellowish green. GC analysis revealed the formation of Cp_2Fe in 90% yield and biphenyl in 80% yield. After removal of the volatiles, the residue was washed with toluene (2 mL × 3) and *n*-hexane (2 mL × 3), extracted with diethyl ether (3 mL), and filtered. Slow evaporation of diethyl ether afforded $[(IPr_2Me_2)_2Fe(PMe_3)_2][BAr^F_4]$ (**4**) as yellowish green crystals (230 mg, 81%). Probably due to the lability of the coordinated phosphine ligand, satisfactory elemental analysis data could not be obtained after several attempts. Anal. Calcd for $C_{60}H_{70}BF_{24}FeN_4P_2$: C, 50.33; H, 4.93; N, 3.91. Found: C, 49.64; H, 4.72; N, 4.03. Absorption spectrum (THF): λ_{max}, nm (ε, M^{-1} cm^{-1}) 315 (6800), 580 (350), 895 (570), 1131 (830), 1537 (270). The ^1H NMR spectrum of this paramagnetic complex displayed six characteristic peaks in the range +150 to −150 ppm in C_6D_6 and THF-d_8. ^1H NMR (300 MHz, C_6D_6/THF-d_8 5/1, 302 K): δ (ppm) 78.41, 24.56, 17.70, 8.07, 7.59, 5.07. Magnetic susceptibility (THF-d_8, 302 K): μ_{eff} = 4.3(1) μ_B.

Reaction of (*p*-tolyl)MgBr with *n*-$C_8H_{17}Br$ Catalyzed by 1. **1** (28.5 mg, 0.05 mmol), *n*-dodecane (0.50 mmol), and *n*-$C_8H_{17}Br$ (1.0 mmol) were mixed at room temperature in diethyl ether (1 mL). A diethyl ether solution of *p*-tolylMgBr (1.0 M, 1.5 mL, 1.5 mmol) was then added in one portion. The entire volume of the reaction mixture was ca. 2.5 mL. Immediately, the mixture turned from yellow to red-brown (Figure S10, Supporting Information). After it was stirred for 5 min at room temperature, the reaction mixture was quenched with water, extracted with diethyl ether (1.0 mL), dried over $MgSO_4$, and analyzed by GC. Yields: *n*-C_8H_{17}(tolyl-*p*), 0.49 mmol (49%); *n*-octane, 0.12 mmol (12%); octenes, 0.22 mmol (22%); *p*-tolyl−tolyl-*p*, 0.22 mmol.

Reaction of (*p*-tolyl)MgBr with *n*-$C_8H_{17}Br$ Catalyzed by $[(IPr_2Me_2)_2FeCl_2]$. The reaction was carried out with $[(IPr_2Me_2)_2FeCl_2]$ (24.5 mg, 0.05 mmol), *n*-dodecane (0.50 mmol), *n*-$C_8H_{17}Br$ (1.0 mmol), and (*p*-tolyl)MgBr (1.0 M, 1.5 mL, 1.5 mmol) in diethyl ether (1 mL) using procedures and reaction time similar to those described above. The entire volume of the reaction mixture was ca. 2.5 mL. A similar color change from yellow to red-brown was observed (Figure S10, Supporting Information). Yields: *n*-C_8H_{17}(tolyl-*p*), 0.47 mmol (47%); *n*-octane, 0.16 mmol (16%); octenes, 0.19 mmol (19%); *p*-tolyl−tolyl-*p*, 0.27 mmol.

Reaction of (*p*-tolyl)MgBr with *n*-$C_8H_{17}Br$ Catalyzed by 4. The reaction was carried out with **4** (72.0 mg, 0.05 mmol), *n*-dodecane (0.50 mmol), *n*-$C_8H_{17}Br$ (1.0 mmol, 1.0 mL), and (*p*-tolyl)MgBr (1.0 M, 1.5 mL, 1.5 mmol) in diethyl ether (1 mL) using procedures and reaction time similar to those described above. The entire volume of the reaction mixture was ca. 2.5 mL. A similar color change from yellow to red-brown was observed (Figure S10, Supporting Information). Yields: *n*-C_8H_{17}(tolyl-*p*), 0.09 mmol (9%); *n*-octane, 0.18 mmol (18%); octenes, 0.35 mmol (35%); *n*-hexadecane, 0.09 mmol (18%); *p*-tolyl−tolyl-*p*, 0.28 mmol.

Reaction of (*p*-tolyl)MgBr with *n*-$C_8H_{17}Br$ Catalyzed by 1 in the Presence of PMe_3. The reaction was carried out with **1** (72.0 mg, 0.05 mmol), PMe_3 (19 mg, 0.25 mmol), *n*-dodecane (0.50 mmol), *n*-$C_8H_{17}Br$ (1.0 mmol), and (*p*-tolyl)MgBr (1.0 M, 1.5 mL, 1.5 mmol) in diethyl ether (1 mL) using procedures and reaction time similar to those described above. The entire volume of the reaction mixture was ca. 2.5 mL. A similar color change from yellow to red-brown was observed. Yields: *n*-C_8H_{17}(tolyl-*p*), 0.08 mmol (8%); *n*-octane, 0.18 mmol (18%); octenes, 0.32 mmol (32%); *n*-hexadecane, 0.09 mmol (18%); *p*-tolyl−tolyl-*p*, 0.27 mmol.

■ ASSOCIATED CONTENT

Supporting Information

Figures, tables, and CIF files giving X-ray crystallographic data, absorption spectra, NMR spectra, a cyclic voltammogram of **1**, photographs of the cross-coupling reactions, and GC graphs of selected reactions. This material is available free of charge via the Internet at http://pubs.acs.org.

■ AUTHOR INFORMATION

Corresponding Author

*E-mail for L.D.: deng@sioc.ac.cn.

Notes

The authors declare no competing financial interest.

■ ACKNOWLEDGMENTS

We acknowledge financial support from the National Basic Research Program of China (973 Program, No. 2011CB808705), the National Natural Science Foundation of China (Nos. 21222208, 21421091, and 21432001), and the Chinese Academy of Sciences.

■ REFERENCES

(1) For monographs and reviews, see: (a) Bolm, C.; Legros, J.; Paih, J. L.; Zani, L. *Chem. Rev.* **2004**, *104*, 6217. (b) *Iron Catalysis in Organic Chemistry: Reaction and Application*; Plietker, B., Ed.; Wiley-VCH: Weinheim, Germany, 2008. (c) Sherry, B. D.; Fürstner, A. *Acc. Chem. Res.* **2008**, *41*, 1500. (d) Czaplik, W. M.; Mayer, M.; Cvengroš, J.; Jacobi von Wangelin, A. *ChemSusChem* **2009**, *2*, 396. (e) Jegelka, M.; Plietker, B. *Top. Organomet. Chem.* **2011**, *33*, 177. (f) Jahn, U. *Top. Curr. Chem.* **2012**, *320*, 191.

(2) For examples, see: (a) Fürstner, A.; Leitner, A.; Méndez, M.; Krause, H. *J. Am. Chem. Soc.* **2002**, *124*, 13856. (b) Nakamura, M.; Matsuo, K.; Ito, S.; Nakamura, E. *J. Am. Chem. Soc.* **2004**, *126*, 3686. (c) Cahiez, G.; Habiak, V.; Duplais, C.; Moyeux, A. *Angew. Chem., Int. Ed.* **2007**, *46*, 4364. (d) Hatakeyama, T.; Hashimoto, S.; Ishizuka, K.; Nakamura, M. *J. Am. Chem. Soc.* **2009**, *131*, 11949. (e) Wunderlich, S. H.; Knochel, P. *Angew. Chem., Int. Ed.* **2009**, *48*, 9717. (f) Adams, C. J.; Bedford, R. B.; Carter, E.; Gower, N. J.; Haddow, M. F.; Harvey, J. N.; Huwe, M.; Cartes, M. Á.; Mansell, S. M.; Mendoza, C.; Murphy, D. M.; Neeve, E. C.; Nunn, J. *J. Am. Chem. Soc.* **2012**, *134*, 10333. (g) Gülak, S.; Jacobi von Wangelin, A. *Angew. Chem., Int. Ed.* **2012**, *51*, 1357.

(3) Fürstner, A.; Martin, R.; Krause, H.; Seidel, G.; Goddard, R.; Lehmann, C. W. *J. Am. Chem. Soc.* **2008**, *130*, 8773.

(4) (a) Noda, D.; Sunada, Y.; Hatakeyama, T.; Nakamura, M.; Nagashima, H. *J. Am. Chem. Soc.* **2009**, *131*, 6078. (b) Sun, C.-L.; Krause, H.; Fürstner, A. *Adv. Synth. Catal.* **2014**, *356*, 1281. (c) Daifuku, S. L.; Al-Afyouni, M. H.; Snyder, B. E. R.; Kneebone, J. L.; Neidig, M. L. *J. Am. Chem. Soc.* **2014**, *136*, 9132.

(5) Bedford, R. B.; Brenner, P. B.; Carter, E.; Cogswell, P. M.; Haddow, M. F.; Harvey, J. N.; Murphy, D. M.; Nunn, J.; Woodall, C. H. *Angew. Chem., Int. Ed.* **2014**, *53*, 1804.

(6) Power et al. have done pioneering studies on bulky aryl iron compounds; see: (a) Power, P. P. *Chem. Rev.* **2012**, *112*, 3482. (b) Kays, D. L. *Dalton Trans.* **2011**, *40*, 769.

(7) For reviews, see: (a) Ingleson, M. J.; Layfield, R. A. *Chem. Commun.* **2012**, *48*, 3579. (b) Bézier, D.; Sortais, J.-B.; Darcel, C. *Adv. Synth. Catal.* **2013**, *355*, 19. (c) Riener, K.; Haslinger, S.; Raba, A.; Högerl, M. P.; Cokoja, M.; Herrmann, W. A.; Kühn, F. E. *Chem. Rev.* **2014**, *114*, 5215.

(8) For examples, see: (a) Bedford, R. B.; Betham, M.; Bruce, D. W.; Danopoulos, A. A.; Frost, R. M.; Hird, M. *J. Org. Chem.* **2006**, *71*, 1104. (b) Gao, H.-H.; Yan, C.-H.; Tao, X.-P.; Xia, Y.; Sun, H.-M.; Shen, Q.; Zhang, Y. *Organometallics* **2010**, *29*, 4189. (c) Ghorai, S. K.; Jin, M.; Hatakeyama, T.; Nakamura, M. *Org. Lett.* **2012**, *14*, 1066. (d) Guisán-Ceinos, M.; Tato, F.; Buñuel, E.; Calle, P.; Cárdenas, D. J. *Chem. Sci.* **2013**, *4*, 1098.

(9) (a) Xiang, L.; Xiao, J.; Deng, L. *Organometallics* **2011**, *30*, 2018. (b) Liu, Y.; Shi, M.; Deng, L. *Organometallics* **2014**, *33*, 5660.

(10) In addition to **1**, a trace amount of orange crystals was also isolated from the reaction mixture. An X-ray diffraction study established its structure as *trans*-$[(\mathrm{IPr_2Me_2})_2\mathrm{FePh_2}]\cdot 0.5\mathrm{C_6H_6}$ (**5**; see the Supporting Information). However, its low yield made further characterization difficult.

(11) For recent examples on iron-NHC compounds, see refs 7 and 9 and: (a) Ohki, Y.; Hatanaka, T.; Tatsumi, K. *J. Am. Chem. Soc.* **2008**, *130*, 17174. (b) Zlatogorsky, S.; Muryn, C. A.; Tuna, F.; Evans, D. J.; Ingleson, M. J. *Organometallics* **2011**, *30*, 4974. (c) Meyer, S.; Orben, C. M.; Demeshko, S.; Dechert, S.; Meyer, F. *Organometallics* **2011**, *30*, 6692. (d) Przyojski, J. A.; Arman, H. D.; Tonzetich, Z. J. *Organometallics* **2012**, *31*, 3264. (e) Hashimoto, T.; Urban, S.; Hoshino, R.; Ohki, Y.; Tatsumi, K.; Glorius, F. *Organometallics* **2012**, *31*, 4474. (f) Blom, B.; Tan, G.; Enthaler, S.; Inoue, S.; Epping, J. D.; Driess, M. *J. Am. Chem. Soc.* **2013**, *135*, 18108. (g) Li, H.; Misal Castro, L. C.; Zheng, J.; Roisnel, T.; Dorcet, V.; Sortais, J.-B.; Darcel, C. *Angew. Chem., Int. Ed.* **2013**, *52*, 8045. (h) Ouyang, Z.; Deng, L. *Organometallics* **2013**, *32*, 7268. (i) Day, B. M.; Pugh, T.; Hendriks, D.; Guerra, C. F.; Evans, D. J.; Bickelhaupt, F. M.; Layfield, R. A. *J. Am. Chem. Soc.* **2013**, *135*, 13338. (j) Hatanaka, T.; Ohki, Y.; Tatsumi, K. *Angew. Chem., Int. Ed.* **2014**, *53*, 2727.

(12) The magnetic susceptibility data measured at lower temperature are difficult to fit due to probably the presence of a paramagnetic impurity formed from hydrolysis or oxidation of **1** by fortuitious moisture or oxidizing species.

(13) Hawrelak, E. J.; Bernskoetter, W. H.; Lobkovsky, E.; Yee, G. T.; Bill, E.; Chirik, P. J. *Inorg. Chem.* **2005**, *44*, 3103.

(14) Vogel, C.; Heinemann, F. W.; Sutter, J.; Anthon, C.; Meyer, K. *Angew. Chem., Int. Ed.* **2008**, *47*, 2681.

(15) For the GC yields of the organic products versus time, please see the Supporting Information.

(16) (a) Smith, R. S.; Kochi, J. K. *J. Org. Chem.* **1976**, *41*, 502. (b) Kleimark, J.; Hedström, A.; Larsson, P.-F.; Johansson, C.; Norrby, P.-O. *ChemCatChem* **2009**, *1*, 152. (c) Hedström, A.; Bollmann, U.; Bravidor, J.; Norrby, P.-O. *Chem. Eur. J.* **2011**, *17*, 11991. (d) Weber, K.; Schnöckelborg, E.-M.; Wolf, R. *ChemCatChem.* **2011**, *3*, 1572. (e) Hedström, A.; Lindstedt, E.; Norrby, P.-O. *J. Organomet. Chem.* **2013**, *748*, 51.

(17) For an excellent review on the role of olefin on metal-catalyzed cross-coupling reactions, see: Johnson, J. B.; Rovis, T. *Angew. Chem., Int. Ed.* **2008**, *47*, 840.

(18) Such type of reductive elimination may be involved in Jacobi von Wangelin's iron-catalyzed cross-coupling of chlorostyrene with phenyl Grignard reagents; see ref 2g.

(19) Lavallo, V.; El-Batta, A.; Bertrand, G.; Grubbbs, R. H. *Angew. Chem., Int. Ed.* **2011**, *50*, 268.

(20) Zhang, H.; Ouyang, Z.; Liu, Y.; Zhang, Q.; Wang, L.; Deng, L. *Angew. Chem., Int. Ed.* **2014**, *53*, 8432.

(21) (a) Andres, H.; Bominaar, E. L.; Smith, J. M.; Eckert, N. A.; Holland, P. L.; Münck, E. *J. Am. Chem. Soc.* **2002**, *124*, 3012. (b) Merrill, W. A.; Stich, T. A.; Brynda, M.; Yeagle, G. J.; Fettinger, J. C.; De Hont, R.; Reiff, W. M.; Schulz, C. E.; Britt, R. D.; Power, P. P. *J. Am. Chem. Soc.* **2009**, *131*, 12693.

(22) Lau, W.; Huffman, J. C.; Kochi, J. K. *Organometallics* **1982**, *1*, 155.

(23) Hendrich, M. P.; Gunderson, W.; Behan, R. K.; Green, M. T.; Mehn, M. P.; Betley, T. A.; Lu, C. C.; Peters, J. C. *Proc. Natl. Acad. Sci. U.S.A.* **2006**, *103*, 17107.

(24) Nakamura et al. have provided evidence for a radical mechanism in iron-catalyzed cross-coupling reactions of alkyl halides with aryl Grignard reagents upon examining the product pattern; see ref 2b.

(25) *Electrochemical Reactions and Mechanisms in Organic Chemistry*; Grimshaw, J., Ed.; Elsevier: Amsterdam, 2000; p 99.

(26) Hu et al. have recent studied his nickel(II) complex catalyzed cross-coupling reaction of alkyl Grignard reagents with alkyl halides in detail and revealed that a bimetallic oxidative addition pathway is preferred for the catalytic system. See: Breitenfeld, J.; Ruiz, J.; Wordrich, M.; Hu, X. *J. Am. Chem. Soc.* **2013**, *135*, 12004.

(27) For photographs of the coupling reactions, please see Figures S10 and S11 in the Supporting Information.

(28) Louie, J.; Grubbs, R. H. *Chem. Commun.* **2000**, 1479.

(29) (a) Chávez, I.; Alvarez-Carena, A.; Molins, E.; Roig, A.; Maniukiewicz, W.; Arancibia, A.; Arancibia, V.; Brand, H.; Manríquez, J. M. *J. Organomet. Chem.* **2000**, *601*, 126. (b) Brookhart, M.; Grant, B.; Volpe, A. F., Jr. *Organometallics* **1992**, *11*, 3920.

(30) (a) Evans, D. F. *J. Chem. Soc.* **1959**, 2003. (b) Sur, S. K. *J. Magn. Reson.* **1989**, *82*, 169.

(31) Sheldrick, G. M. *SADABS: Program for Empirical Absorption Correction of Area Detector Data*; University of Göttingen, Göttingen, Germany, 1996.

(32) Sheldrick, G. M. *SHELXTL 5.10 for Windows NT: Structure Determination Software Programs*; Bruker Analytical X-ray Systems, Inc., Madison, WI, USA, 1997.